

## MEASUREMENT OF DRAG AND LIFT FORCE OF A HOLLOW PROJECTILE UNDER DIFFERENT WIND CONDITIONS

M. Nasir Uddin<sup>1\*</sup>, Md. Humayun Kabir Bhuiyan<sup>2</sup> and M. Qamrul Islam<sup>3</sup>

<sup>1,2,3</sup>Department of ME, Military Institute of Science and Technology, Dhaka, Bangladesh.

Article Received on 10/06/2020

Article Revised on 30/06/2020

Article Accepted on 20/07/2020

### \*Corresponding Author

M. Nasir Uddin

Department of ME, Military  
Institute of Science and  
Technology, Dhaka,  
Bangladesh.

### ABSTRACT

The hollow projectile known as a tubular projectile is an important parameter to be considered to improve its performance characteristics greatly. The design parameters of a projectile depend on the drag and lift forces acting on the projectile. Therefore, a detail experimental and simulation are required to understand the projectile performance

against the wind. In this study, experimental and numerical investigations of a hollow shape projectile under different wind conditions are carried out. Here a 105 mm hollow shape projectile is used in while performing the experiment. The experiment is carried out by placing the projectile in front of the wind tunnel. The simulation was done using software at an Angle of Attack (AOA) 45°, keeping wind velocity and geometry the same. The pressure coefficients were calculated from the measured values of the surface static pressure distribution on the projectile. The drag and lift coefficients were further obtained from the measured pressure and a projected area of the projectiles. The wind flow effect on the projectiles was also analysed by ANSYS software. The simulation and experimental result show similar trend regarding drag and lift forces.

**KEYWORDS:** *Projectile, long range, CFD, Drag Force, Lift Force.*

### INTRODUCTION

Due to the large use of long-range projectiles worldwide, the study of aerodynamic characteristics of projectiles has become one of the most important focuses for its improvement. Within the field of projectile design, there has been a frequent endeavouring to

increase the range and precision target hitting of projectiles [Bolokin, 2013., Suliman *et al.*, 2009., and Sahu, 2003.,]. The increased range is achieved by the performance improvement of the projectiles. However, the forecast of drag coefficients and lift coefficients for diverse formations are crucial. However, various parameters such as fins and jets can be utilized to increase aerodynamic characteristics for better control on manoeuvring projectile. Hence, several research works have been carried out by using various smart technology to improve the performance of the projectiles [Sahoo *et al.*, 2014, Novak *et al.*, 2018., and Wessam *et al.*, 2014.,]. Self-adaptive ballistic correction is considered as an important parameter nowadays by applying numerous advanced intelligent control [Wessam *et al.*, 2014.,]. Besides, stability and optimization of projectiles are the significant factors for the flight performance by reducing drag [Yongie *et al.*, 2015., Linj *et al.*, 2018.,]. They have noted that inadequate system stability outcomes in the failure of operations. Moreover, the long ranges and precise target hitting by a projectile are projected to be persistently enriched, particularly when a new projectile is developed or an existing projectile is modified or upgraded [Linj *et al.*, 2018.,]. Consecutively, the hollow projectile known as a tubular projectile is an important parameter to be considered to improve its performance characteristics greatly [Dali *et al.*, 2019.,]. Research on optimal hollow projectile shows that the bow shock wave in front of it results in the projectile drag coefficient reductions abruptly. Furthermore, ballistic projectile precision depends on measurement structures for the location which can be determined by using gravity vector estimation. Therefore, this study forecasts on the investigation of projectiles under different wind conditions. The demonstration is being performed to investigate the effect of design parameters on the system performance of the projectile and its effective flight path.

### ***A. Motivation***

Smart, intelligent, and high mobility of ammunition is the important development direction of ammunition technology in a long historical period. In the future, self-adaptive ballistic correction and autonomous attack smart ammunition by applying various innovative intelligent control technology have become the research focus of the world's national defense science and technology.

One of the most important aerodynamic performance characteristics for the projectile's shell is the total drag. The total drag for projectiles can be divided into three components: (i) pressure drag (excluding the base), (ii) viscous (skin friction) drag, and (iii) base drag. The base drag is a major contributor to the total drag, particularly at the transonic speeds. Thus, the minimization

of base drag is essential in minimizing the total drag of projectiles. The breakdown of the total drag into various components is important in the preliminary design stage of a shell. This information can aid the designer to find potential areas for drag reduction and achieve the desired increase in range and/or terminal velocity of projectiles since they are affected by the projectile drag.

Due to the rapid development of the Field Artillery Weapon system over time, many researchers have worked on this topic to increase the range and accuracy of the projectiles. Ever-increasing demands for accuracy and range in modern warfare have expedited the optimization of a projectile design. The crux of projectile design lies in the understanding of its aerodynamic properties early in the design phase.

Therefore, studying the projectile based on their sizes, shapes, air velocity, and Angle of Attack of the Airstream seems an important parameter to optimize the design of a projectile.

### ***B. The Effect of wind on Projectile***

The effect of wind on the projectiles as a whole is determined by the combined action of external and internal pressures acting upon it. In all cases, the calculated wind loads act normal to the surface to which they apply. The pressures created inside a hollow shape projectile due to access to wind through openings could be suction (negative) or pressure (positive) of the same order of intensity while those outsides may also vary in magnitude with possible reversals. Thus, the design value shall be taken as the algebraic sum of the two inappropriate/concerned direction. Furthermore, the external pressures (or forces) acting on different parts of a projectile do not correlate fully. Hence, there is a reduction in the overall effect.

The development of modern materials and construction techniques has resulted in the emergence of a new generation of projectiles. Such projectiles exhibit increased susceptibility to the action of wind. Accordingly, it has become necessary to develop tools enabling the designer to estimate wind effects with a higher degree of refinement than has been previously required. It is the task of the engineer to ensure that the performance of projectiles subjected to the action of wind will be adequate during their anticipated flight path from the standpoint. To achieve this end, the designer needs information regarding (i) the wind environment, (ii) the relation between that environment and the forces it induces on the structures, and (iii) the behavior of the projectiles under the action of forces.

Since all wind loadings are time-dependent because of varying speeds and direction of winds, wind loading is never steady. For this reason, the static load is referred to as the steady (time-variant) forces and pressures tending to give the projectiles a steady displacement. On the other hand, the dynamic effect tends to set the structure oscillating. A steady wind load on a projectile is very difficult to achieve. Always wind loads are fluctuating because of varying speeds and directions of winds. The type of wind and the stiffness and roughness of the projectile determine the nature of the effect on a projectile. When a projectile is very stiff the dynamic response of the projectile may be neglected and only the static loads may be considered. This is because the natural frequency of an extremely stiff structure is too high to be excited by the wind. In the present study, the effect of static loading is taken into account due to the steady wind. Since natural winds are continually fluctuating, it is generally assumed that these fluctuations are so irregular and random that the response of a structure will not differ from that due to a steady wind of the same average speed.

### *C. The Necessity of the Study*

In recent years the hollow projectile research development has become one of the main projectiles in small caliber artillery researches. The circular duct along the longitudinal axis of the hollow projectile which causes high muzzle velocity and low drag makes its performance characteristics greatly improved. The characteristics, such as a flat trajectory and short flight time caused by high flight velocity, spin stabilization can ensure the high accuracy and low dispersion of hollow projectile. Also, the hollow projectile has good performance characteristics, such as superior target penetration, The extended firing ranges and impact precision of weapons systems are expected to be constantly improved, especially when new ammunition is developed or when existing ammunition is modified. Aerodynamic bodies such as projectiles, missiles, and rockets generally, undergo deterioration of flight performance by drag and it affects a projectile. The base drag frequently accounts for one-half, or even much more, of the total drag for large caliber ammunition. Reducing the base drag is an efficient and practical way to reduce the total drag of projectile, and increase the range of projectile for up to 30%. Within the field of artillery techniques, there has been a continual striving to increase the range and precision of field guns. Increased range is achieved either by gun improvements, which even include modifications to propellant charges such that redesign of gun parts is required due to for example increased gas pressure in the barrel, or by improvements in the projectile performance. Improved projectile performance can be achieved in several different ways which to a certain extent can be combined in the same projectile. Base drag contributes

generally to a relatively large part of the total drag and depends upon the fact that the base pressure due to the resulting wake flow in the base region is lower than the ambient air pressure.

There are roughly four classes of techniques to predict aerodynamic forces and moments on a projectile in atmospheric flight: empirical methods, wind tunnel testing, computational fluid dynamics simulation, and spark range testing. In computational fluid dynamics (CFD) simulation, the fundamental fluid dynamic equations are numerically solved for a specific configuration. The most sophisticated computer codes are capable of unsteady time-accurate computations using the Navier-Stokes equations. The prediction of aerodynamic coefficients for projectile configurations is essential in assessing the performance of new designs.

The coefficient of drag is an important parameter in external ballistics. A 130 mm artillery shell at 943 m/s muzzle velocity in vacuum covers a maximum range of 90.7 km whereas, in the presence of air, its range reduces to 24 km. Therefore, the coefficient of drag plays a vital role in the case of range and depends strongly on the shape of the nose of the projectile. The major work of the flight engineer is to calculate the drag of flight for various speeds, altitudes, and different design configurations and try to analyze, how it can be reduced to increase the performance. It is the main drawback because to go through all that it's very difficult task forces will be different on different configurations for different parameters. For predicting the lift and drag coefficients we need a deliberate study of a projectile under different wind conditions.

Differences between the wind tunnel and the full-scale result can occur due to Reynolds's number inequality, incorrect simulation of the atmospheric boundary layer, and the small-scale difference between wind tunnel and the prototype model. In most wind tunnels tests the full-scale Reynolds number is rarely achieved. Boundary layer separation depends on the Reynolds number. For sharp-edged structures, separation point does not depend on Reynolds number. On the other hand, the flow field around curved surfaces are very much Reynolds number dependent, so tests on these configurations must be treated with care the crosswind scales in wind tunnels are often less-than reality. This can cause underestimation of crosswind effects. The scale difference between the wind tunnel model and prototype is found in the high-frequency fluctuation. High peaks found on the cladding in full-scale are not found in the wind tunnel. Those effects may be caused by structural details that are not simulated in the wind tunnel model.

Nowadays, both the studies with models and projectiles are being performed to compare the result for verifying the validity of the former. But full-scale experiments are both costly and difficult to perform. For the present study with different projectiles, full-scale experiments will not only be complex and costly but also it would be difficult to record reliable pressure distribution simultaneously on the single as well as group of the projectile as there will be a variation of speeds and direction of the wind with time. The flow around projectiles in the actual environment is very complex and formulation of a mathematical model to predict the flow is almost impossible. Thus, the model study is a must and the results obtained under the simulated condition in the laboratory are found to be quite satisfactory for practical purposes.

#### ***D. The Objective of This Study***

In the present investigation a hollow shape projectile like 105 mm has been taken into consideration. The objectives of the study are:

- (i) To measure the lift and drag force of a projectile depending on the angle of attack and therefore, the effect of the trajectory of a projectile using a subsonic wind tunnel.
- (ii) Numerical modeling of lift and drag coefficient for wind flow over the projectile.
- (iii) Validation of numerical modeling using experimental data.
- (iv) Recommendation for modification of existing projectile design.

The results **have been** expressed in non-dimensional parameters, so that it may be applied for different types of prototype projectiles. The findings enable the engineers to design different special projectiles effectively.

## **2. EXPERIMENTAL SETUP AND CONDITIONS**

The research has been carried out based on a theoretical analysis for a small scale projectile along with the formulation of the mathematical model and numerical analysis. The mathematical model has been formulated by understanding the wind nature, analyzing the mechanics of projectile-wind interaction, and the interaction of air-flow-aerodynamics. The selected projectile is then used for simulating the system performance, optimizing the design parameters, and effective range. The optimized design parameters are used for developing a numerical model and relationship between lift coefficients and drag coefficients with free stream velocities and angle of attacks with the help of ANSYS software.

The experiment has been conducted in an open circuit subsonic wind tunnel installed at Mechanical Fluid Mechanics Laboratory in MIST. The successive sections of the wind tunnel

comprise a bell mouth entry, a flow straightener, a diverging section, and two axial flow fans. Flow along the central longitudinal axis of the wind tunnel has been maintained at a constant height from the floor. The hollow projectile was placed at the exit end of the wind tunnel. A hollow shape projectile (105 mm) has been developed for the experiment. Here the static pressure measurement of hollow shape projectile was done at 45 degree Angle of attack. Finally, the performance parameters of the developed shell model have been investigated experimentally and numerically.

### A. Experimental Conditions

A 105 mm hollow shape projectile at 45 degree Angle of Attack (AOA) is used. The number of tapping points around the projectile was 30. The static pressure was measured at each tapping point with a kerosene manometer. The minimum deflection of the manometer can be measured was 1 mm. The air velocity was 4.7 m/s. The computational fluid dynamics (CFD) simulation was done on similar conditions to compare the experimental and simulation results. The CFD simulation consists with ANSYS Multiphysics Software with a fluent solver.

### B. Test Setup

The test was done in an open circuit subsonic wind tunnel as shown in Figure 1. It was the low-speed wind tunnel having the maximum wind velocity of 6.8 m/s in the test section. The tunnel consists of various components such as fan, valve, silencer, honeycomb, etc. It is 6.16 m long with a test section of 490 mm x 490 mm cross-section. To make the flow.

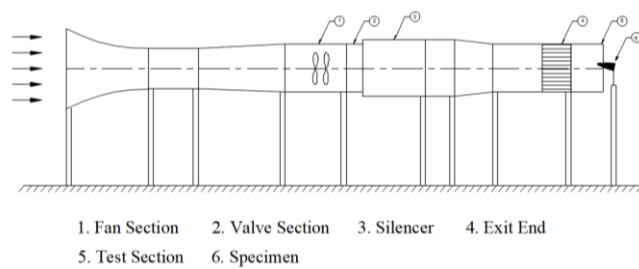


**Figure 1: Schematic diagram of the wind tunnel uniform, a honeycomb was fixed near the end of the wind tunnel. There is a converging bell mouth shaped entry. To generate the wind velocity, two axial flow fans were used.**

Each of the fans is connected with the motor of 2.25 kilowatt and 2900 rpm. There is a regulator to control the wind speed. There is a silencer as shown in Figure 1. The central longitudinal axis of the wind tunnel is maintained at a constant height of 1010 mm from the

floor. The converging mouth entry is incorporated in the wind tunnel for smooth entry of air into the tunnel and to maintain uniform flow into the duct-free from outside disturbances.

A variable frequency drive was used to control the flow. A silencer was fitted at the end of the flow controlling section to reduce the noise of the system. This section was incorporated with a honeycomb. The diverging and converging section of the wind tunnel is 965 mm long and made of 18 GMS black sheets. The angle of divergence and convergence is  $29^\circ$ , which has been done to minimize expansion and contraction loss and reduce the possibility of flow separation.

In each case of the tests, wind velocity was measured directly with the help of a digital anemometer. The flow velocity in the test section was 4.7 m/s approximately. The measured velocity distribution was almost uniform across the tunnel test section in the upstream side of the test models.

In reality, the test was done at the exit end of the wind tunnel in the open air as shown in Figure 1. The projectile is placed with a stand at the same level as the wind tunnel at the exit end. In the middle of the hollow cylinder, it was made groove and connected with a plastic tube. Either side of the plastic tube is connected with an inclined multi-manometer. The circular projectile was equally spaced and made a total of 30 taps. The manometer is made with 30 tubes and connected with projectile grooves. 30 scales were fixed along the 30 tubes in the manometer to take the reading. It is mentionable here that fluid used in each manometer is kerosene with specific gravity of 0.8.

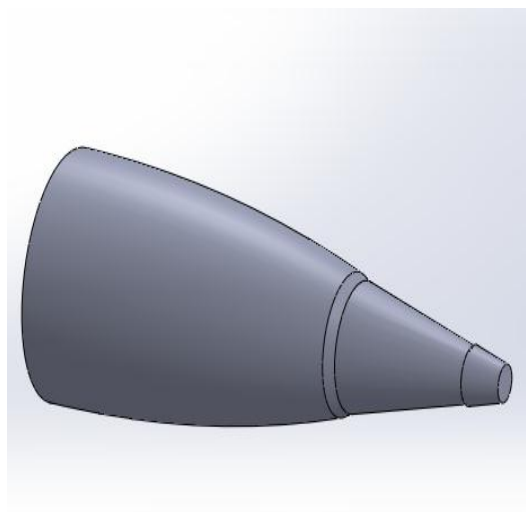
Since the top and bottom of the extended part of the wind tunnel was open; as such no correction for the blockage was done in the analysis. The projectiles were placed very close to the exit end of the wind tunnel so that the approach velocity of a projectile was approximately identical as that in the exit end of the wind tunnel. The projectile is placed at the exit end of the wind tunnel  $45^\circ$  angle of elevation. and necessary data was recorded and subsequently, calculations are carried out.

### ***C. Preparation of the Projectiles***

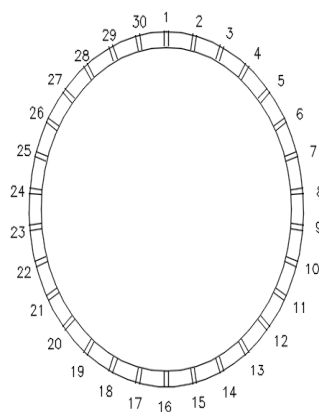
In this experiment one 105 mm projectile has been prepared with seasoned teak wood to avoid the buckling and expansion due to the change of temperature and humidity. The 105 mm projectile is shown in Figure 2(a) and the tapping position is shown in Figure 2(b). The tapping

positions on the cross-section of the cylinder are shown in Figure 2(a) and 2(b). The diameter of the projectile is 105 mm and contained 30 tapings and placed them at an equal angle.

Each tapping was identified by a numerical number from 1 to 30 for each of 105 mm, 122 mm and 130 mm projectiles. The tapping's were made along the circular -section of the projectile. Keeping the outside of the projectiles intact the inside of the projectiles was made hollow through which the plastic tubes were allowed to pass. The plastic tubes were connected with the copper tubes at one side and the other side with the inclined multi-manometer. The manometer liquid was Kerosene. The tapping's were made of copper tubes of 2 mm.



(a)



SECTIONAL VIEW (X-X')

(b)

**Figure 2: (a) 105 mm projectile and (b) the tapping points on it.**



(a)



(b)

**Figure 3: (a) Position of the projectiles against the wind and (b) measurement of the pressure at the tapping points of the projectile outside diameter. Each tapping was of 50 mm length approximately. From the end of the copper tube flexible plastic tube of 1.5 mm, inner diameter was press-fitted. In the experimental investigation, one 105 mm projectile was used where experimental reading was taken placing the single projectile in front of the wind tunnel. Figure 3(a) and 3(b) shows the experimental setup for measuring the pressure on the projectile.**

The wind velocity across the test section of the wind tunnel was measured with the help of a digital anemometer. A pitot tube was also used to measure the velocity to cross-check. The surface static pressures were measured with the help of an inclined manometer. The inclination of the manometer was sufficient to record the pressure with reasonable accuracy.

### 3. MATHEMATICAL MODEL AND SIMULATION

The calculation procedure of finding pressure coefficients, drag, and lift coefficients has been described briefly in this chapter along with the simulation procedure. From the measured surface static pressure on the projectiles are obtained. The air velocity of the air stream is

obtained from the anemometer and the projected area of the segmented part of the projectile is calculated through Solid works modeling. Then the drag( $C_D$ ), lift ( $C_L$ ), and Pressure Coefficient ( $C_P$ ) are calculated.



**Figure 4: Wooden projectiles after manufacturing.**

The design of the Projectile was done through reverse engineering of the real long-range projectiles used in the real battlefield. The Projectiles are manufactured with seasoned wood material in a lathe machine. The holes are made on the surface of the projectiles to measure pressure acting on the projectiles. Figure 4 shows the manufactured projectiles with wood tested in experiment.

The pressure is measured at the tapping is measured by using Equation 1.

$$p = \Delta h_k \rho_k g \quad (1)$$

Where,  $p$  is the pressure ( $N/m^2$ ),  $\Delta h_k$  is the manometer reading,  $\rho_k$  is the density of Kerosene, and  $g$  is the gravitational acceleration.

The acting force on a single segment (assuming segment 1) is calculated from Equation 2.

$$F_1 = p A_{Projected 1} \quad (2)$$

Then the total force acting on the projectile is

$$F = F_1 + F_2 + F_3 \dots \dots + F_{30} \quad (3)$$

As the air is coming at an angle, therefore, the total forces will be divided into horizontal and vertical direction. If the angle of attack is ' $\alpha$ ' then the drag and lift force are calculated from Equation 4 and 5.

$$F_D = F \cos \alpha \quad (4)$$

$$F_L = F \sin \alpha \quad (5)$$

The drag coefficient ( $C_D$ ), lift coefficient ( $C_L$ ), and pressure coefficient ( $C_p$ ) are calculated from Equation 6, 7, and 8.

$$C_D = \frac{2 * F_D}{A_{Total} * \rho_k * U_\infty^2} \quad (6)$$

$$C_L = \frac{2 * F_L}{A_{Total} * \rho_k * U_\infty^2} \quad (7)$$

$$C_p = \frac{\Delta P}{\frac{1}{2} \rho_{air} U_\infty^2} \quad (8)$$

Where,  $\Delta P = P - P_0$ ,  $P$  is the static pressure on the surface of the projectile,  $P_0$  is the ambient pressure,  $\rho_{air}$  is the density of the air,  $U_\infty$  is the free stream velocity, and  $A_{Total}$  is total Active projected area ( $A_1 + A_2 + A_3 + \dots \dots + A_n$ ).

The projected area for each segment is calculated from the Solid works model. The projectiles are segmented into 30 strips and then a 3D drawing was drawn to connect the top and bottom of the projectiles. Then a 2D drawing was drawn on a plane facing the air stream. The area of all segments was not calculated as they can not be seen from the front of the plane facing the wind. Therefore, the pressure difference in those areas is fluctuating due to turbulence and not dependable. Figures 5, 6, and 7 show the projected area measurement by SolidWorks.

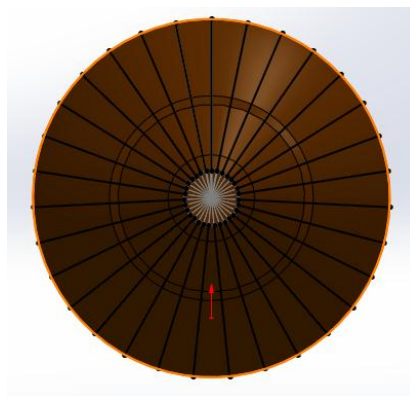


**Figure 5: Plan view of the projectile from air direction.**

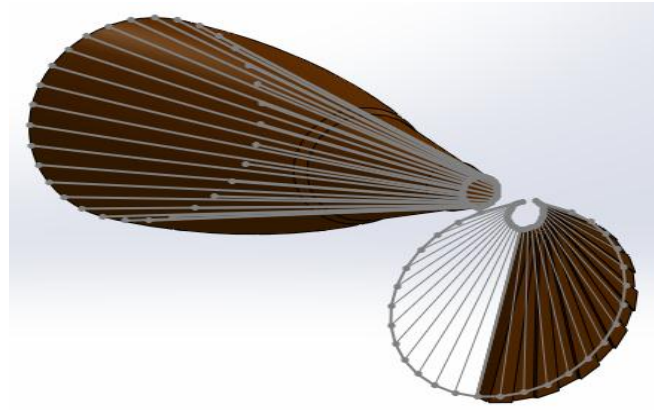


**Figure 6: Area drawn from the projection of the segments.**

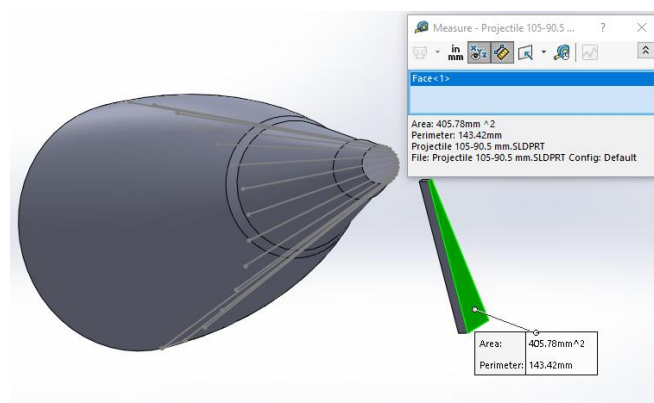


**Figure 7: Measurement of the projected area.**

Computational fluid simulation is done on all the projectile according to the experimental conditions. ANSYS software is used to analyse the CFD model. The Solid Works model made for measuring the projected area is used for simulation. The projectile is considered as a solid domain and outside of it is considered as air domain. The k-e turbulence model is used for solving the problem. The inlet condition was 4.7 m/s air and outlet condition was atmospheric condition similar to experiment. The rest of the surface is considered as wall. Figure 8 shows the geometry of the 105 mm projectile, and the mesh file for simulation is shown in Figure 9.

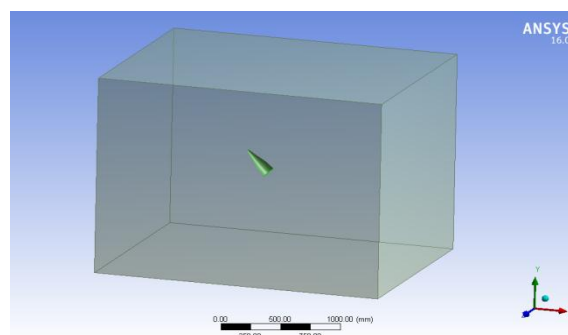


**Figure 8: Geometry files of 105 mm projectile for CFD simulation.**

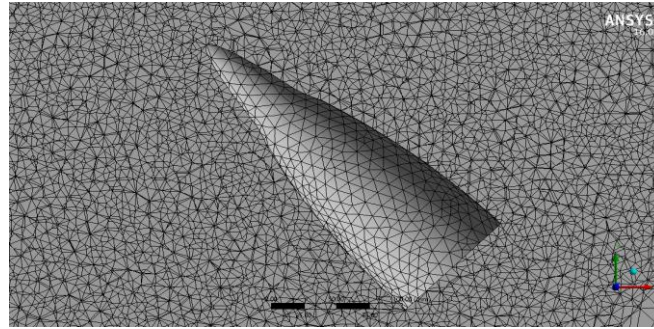


**Figure 9: Mesh of the CFD Simulation for 105 mm Projectile.**

#### **4. RESULTS AND DISCUSSIONS**

The manometer reading was converted into pressure and the total force was calculated based on the segmented area of the projectile. The drag force and lift forces were calculated based on the attack angle. The total drag force and lift force were summed up for the whole projectile and later the lift, drag, and pressure coefficients are calculated.

A set of experiments have been conducted for 105 mm projectile. The projectile was kept at  $45^\circ$  angle with horizontal axis. The projectile is then rotated at various angles to investigate the effect of the wind on the projectile and exerted the drag and lift forces on it. Figure 10 shows the effect of rotation of the projectile relative to the vertical plane. The projected area was calculated through Solid Works. The Left and Right side have same projected area as the projectile is symmetric. Figure 11 shows the projected area as, Front Side, 45 Degree Left, and Back of the Projectile. The Experimental results are shown in the Figure 12 and Tabulated in Table 1. The total forces acting on the projectiles are highest for the side orientation (90 Degree) as the physical size is the largest from this orientation. The minimum forces observed from the front. However, the forces acting in the back could be working in favour of the projectile range due the combined effect of the attack angle of wind, orientation of the projectile, and the firing direction of the projectile.

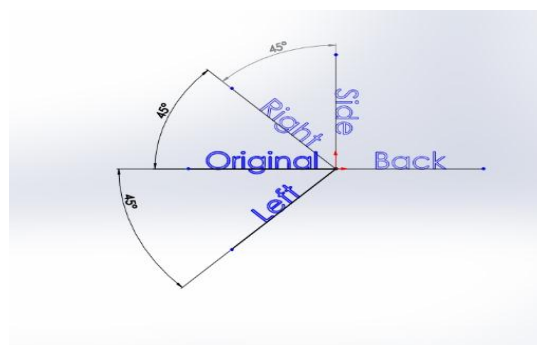
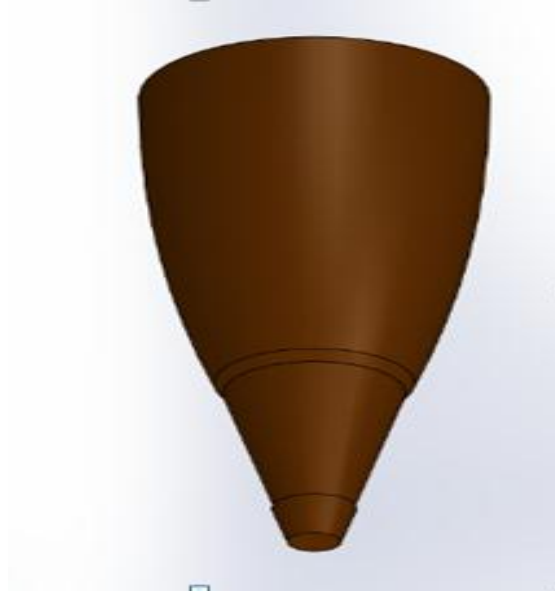
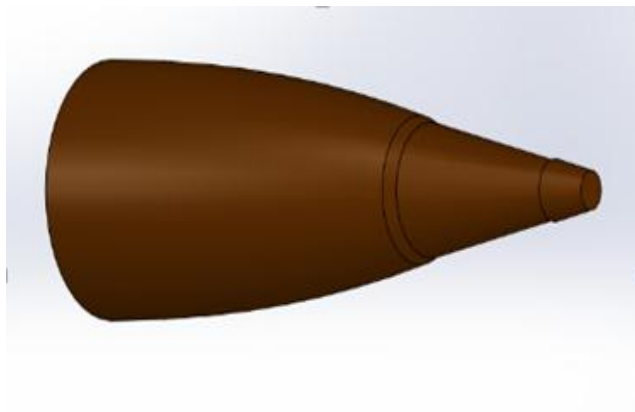


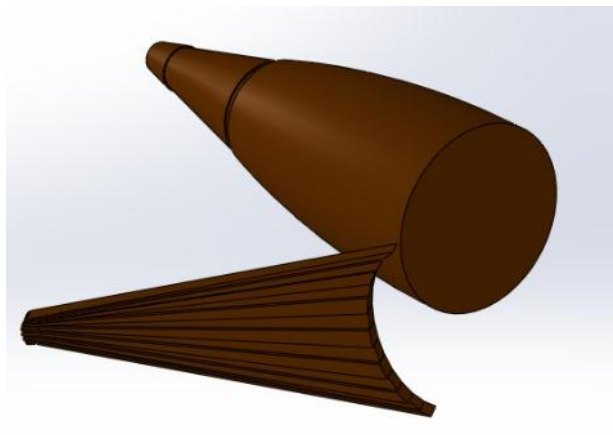
**Figure 10: The rotation of the 105 mm projectile at different angles. (Vertical plane).**



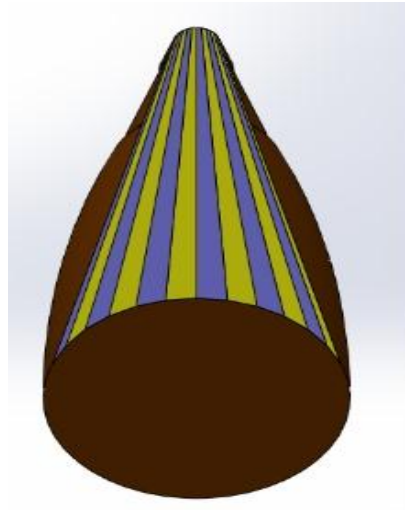
(a)



(b)

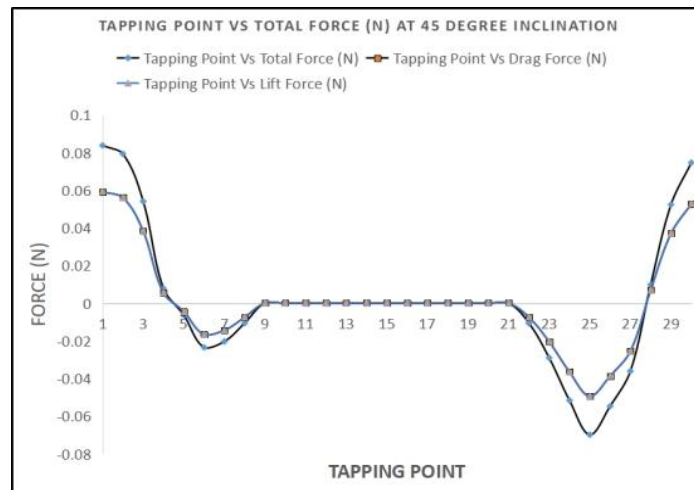


(c)

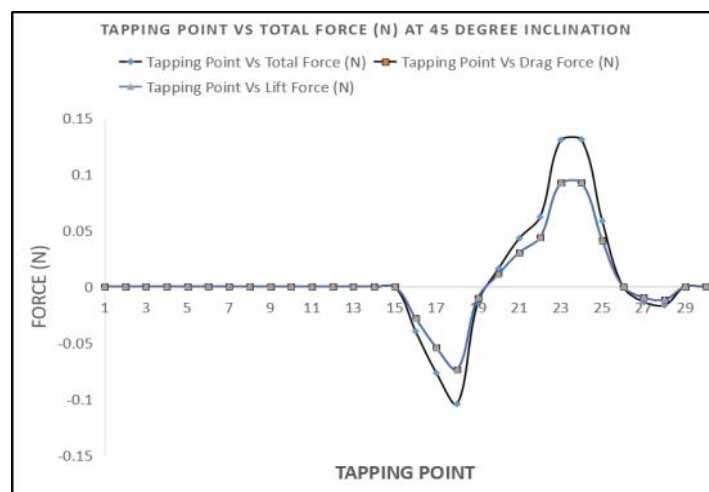


(d)

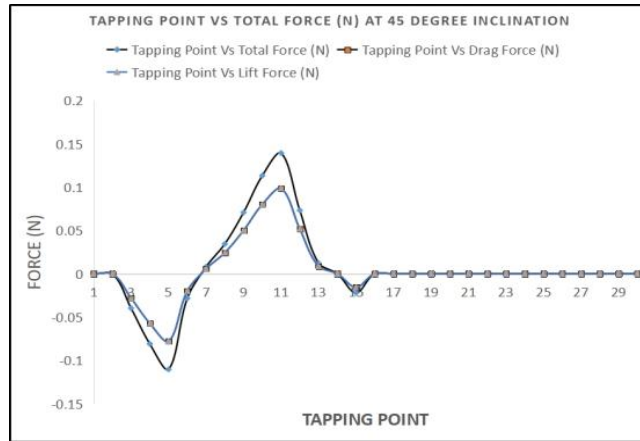
Figure 11: The projected area for (a) Front (b) Side (c) 45 Degree Left, and (d) Back.



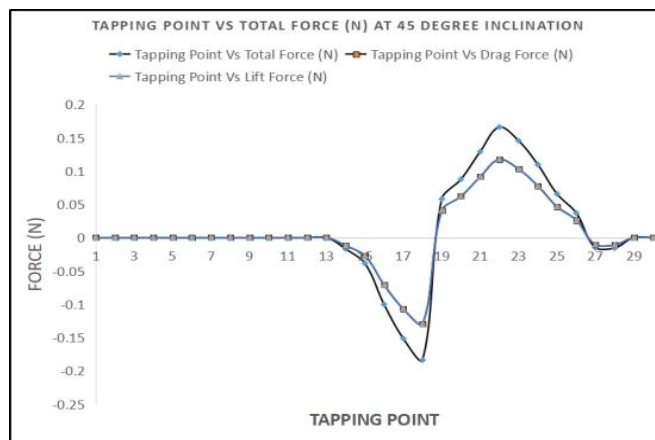
(a) 0° Location (Original Location).



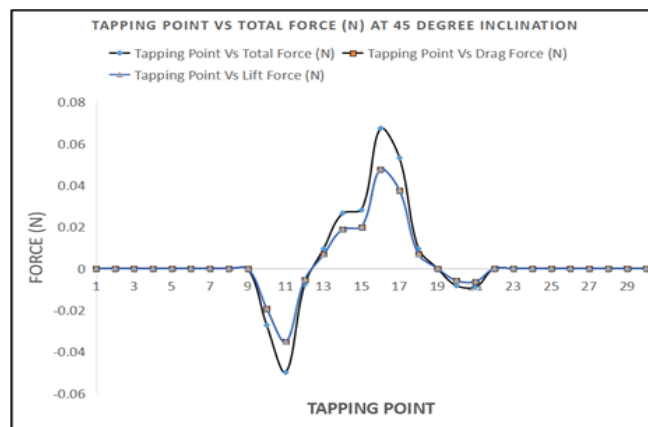
(b) 45° Left



(C) 45° Right



(D) 90° Side



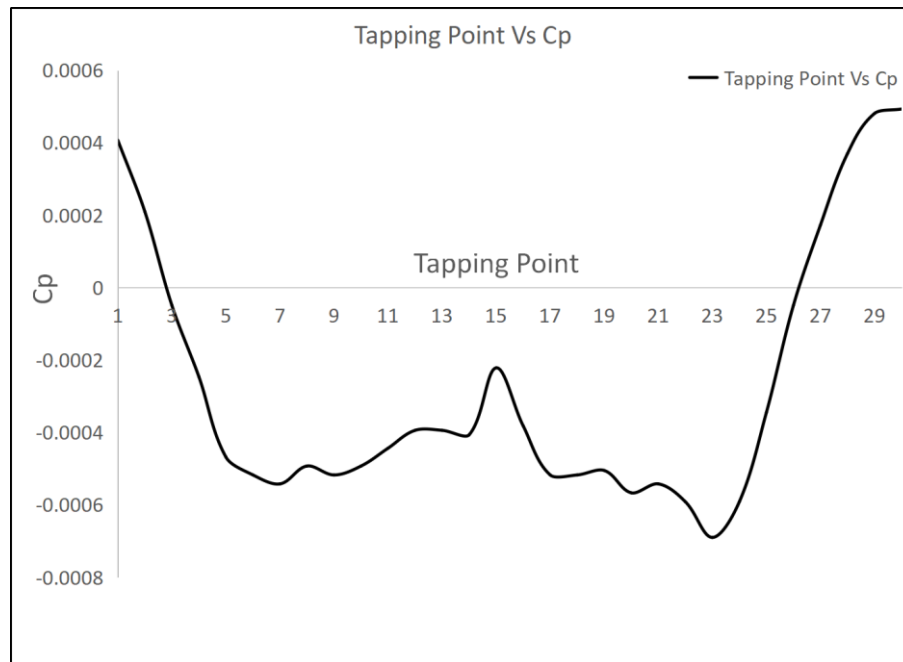
(E) Back (180°)

Figure 12: Forces acting on the Projectile at 45° angle at different orientation.

**Table 1: Total acting forces on 105 mm Projectile at 45 attack angle and for different orientation.**

Test Condition	Projected Area (m <sup>2</sup> )	Total Force (N)
Side (90 Degree)	0.01605171	0.275914084
Oblique Right (45 Degree)	0.0104243	0.169768101
Oblique Left (45 Degree)	0.0104243	0.176007448
Back (180 Degree)	0.00599396	0.091658895
Front (Original 0 Degree)	0.01450555	0.049247828

The pressure coefficient is calculated and plotted against the tapping points on the projectiles. The pressure coefficients at the tapping points that are facing the air gradually decreasing and increasing. The measurement at the back of the projectile is very fluctuating as turbulence was observed in the back. Therefore, the pressure coefficients at the back of the projectile is not dependable.



**Figure 13: Tapping Point Vs Pressure Coefficients for 105 mm Projectile.**

The simulation pressure and velocity gradient are shown for 105 mm, projectile in Figures 14-15. The pressure contour shows that the pressure is more felt at the front of the projectiles. However, the velocity streamline plot shows that the streamline is flowing over the 105mm projectile.

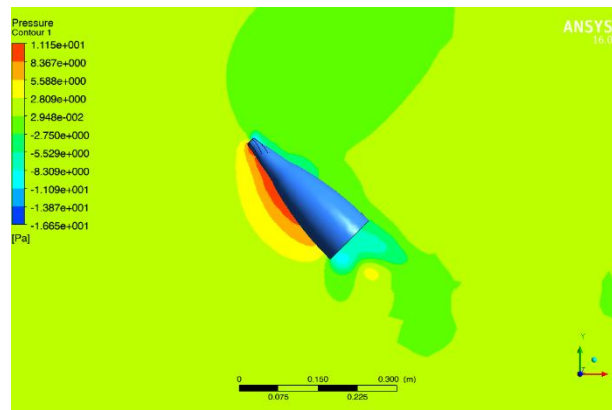


**Figure 14: The pressure contour for 105 mm projectile at 45° AOA.**

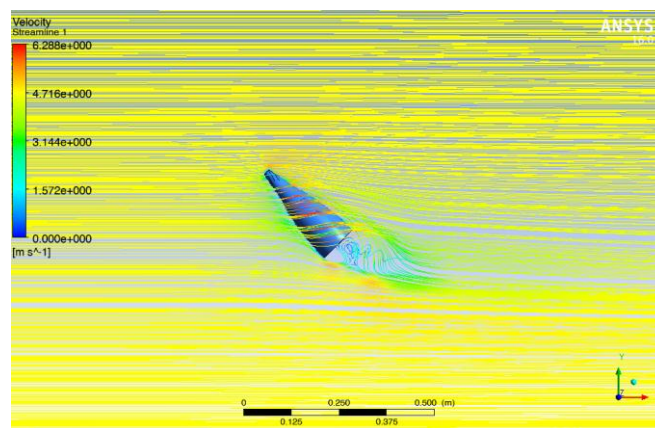


**Figure 15: The velocity contour for 105 mm projectile at 45° AOA**

Figure 12 shows that the drag force and lift force varies according to the rotation of the projectile. Because according to the rotation of the projectile the projected area differs. Accordingly total force differs at various positions of projectiles which are shown in table.

## 5. CONCLUSIONS

During the measurement of the surface static pressures on the projectiles, the room temperature is assumed to be constant. As such the density of the air is taken as constant in the calculation. In reality, there is a minor variation of the temperature during taking all the readings, which has been neglected in the calculation. The fluctuation of the manometer reading was observed especially on the suction side of the cylinders which was not significant. While taking the reading, always the mean value of the manometer was recorded. Since fluctuation was insignificant the error in the measured values was negligible. The scale beside the manometer has a precision of 1.0 mm deflection. Therefore, it was quite difficult to measure the deflection of the kerosene column below 1 mm. However, the specific are as follows:

- (i) The projectiles start at zero velocity, therefore, the experiment conducted at 4.7 m/s provides the initial flight scenario and drag and lift forces related to it.
- (ii) The simulation and experimental results found in this investigation show that the drag force and lift forces varies according to the vertical rotation of the projectile.
- (iii) The experimental results show that the drag force and lift force are increased at the projected area of the projectile that comes in contact with the air directly.
- (iv) The simulation shows that air streamline is flowing over the 105 mm projectile hence decreased the drag forces significantly.
- (v) The pressure contour shows more pressure at the front of the projectiles that come in contact with the air directly, whereas, the pressure at the back of the projectiles only comes in contact with the air due to the turbulence.

Finally, the experimental and simulation results show some diversion which may result from many sources that need to address in future studies.

## ACKNOWLEDGEMENTS

The authors would like to give thanks to Military Institute of Science and Technology (MIST) and the Workshop Division and Fluid Mechanics Lab of Department of Mechanical Engineering, MIST for providing financial support and laboratory facilities.

## REFERENCES

### Journal articles

1. Bolonkin, A., Long Distance Bullets and Shells. *International Journal of Aerospace Sciences*, 2013; 2(2): 29-36.
2. Dali, M. A., and Jaramaz, S., Optimization of Artillery Projectiles Base Drag Reduction using Hot Base Flow, *Thermal Science*, 2019; 23(1): 353-364.
3. Hemateja, A. B., Ravi, Teja., Dileep K.A., Rakesh, S.G. Influence of Nose Radius of Blunt Cones on Drag in Supersonic and Hypersonic Flows. *Material Science and Engineering*, 2017; 225: 012045.
4. Novak, L., Bajcar, T., Širok, B., Orbanić, A., Bizjan, B., Investigation of Vortex Shedding from an Airfoil by Computational Fluid Dynamic Simulation and Computer-Aided Flow Visualization. *Thermal Science*, 2018; 22(6B): 3023-3033.
5. Lijin, J., and Jothi, T. J. S., Aerodynamic Characteristics of an Ogive-nose Spinning Projectile. *Sadhana*, 2018; 43:63: 1-8.

6. Sahoo, S., Laha, M. K., Coefficient of Drag and Trajectory Simulation of 130 mm Supersonic Artillery Shell with Recovery Plug or Fuze. *Defence Science Journal*, 2014; 64(6): 502-508.

### Conference Proceedings

1. Alexey, M.L., Stanislav, A.K., Ivan, G.R., (2017). Optimization of Aerodynamic Form of Projectiles for Solving the Problem of Shooting Range Increasing. AIP Conference Proceeding, 1893; 030085.
2. Suliman, M. A., Mahmoud, O. K., Al-Sanabawy, M.A., Abdel-Hamid, O.E. Computational investigation of base drag reduction for a projectile at different flight regimes. 13<sup>th</sup> International Conference on Aerospace Sciences & Aviation Technology, Paper ASAT-13-FM-05, 2009; 1-13.
3. Sahu, J., (2003), Unsteady numerical simulations of subsonic flow over a projectile with jet interaction. 41<sup>st</sup> Aerospace Sciences Meeting and Exhibit, AIAA, 2003-1352; 1-10.
4. Wessam, M. E., Huang, Z., and Chen, Z., Aerodynamic characteristics and flow field investigations of an optimal hollow projectile. Proceedings of the 5<sup>th</sup> International Conference on Mechanical Engineering and Mechanics, 2014; 181-186.
5. Yongjie, X., Zhijun, W., Guodong, W., Jianya, Y., Shouli, P., Ballistic characteristics of rocket projectile with deflection nose. International Power, Electronics and Materials Engineering Conference (IPEMEC 2015), 2015; 405-41.